

TM-71-1031-3

TECHNICAL MEMORANDUM

CALCULATION OF THE THERMODYNAMIC
STATE OF A
THREE-DIMENSIONAL ATMOSPHERE

Bellcomm



FACILITY FORM 602

N71-34302
(ACCESSION NUMBER)

54
(PAGES)

CR-121745
(NASA CR OR TMX OR AD NUMBER)

(THRU)
G 3

(CODE)
13

(CATEGORY)

COVER SHEET FOR TECHNICAL MEMORANDUM

TITLE- Calculation of the Thermodynamic
State of a Three-dimensional
Atmosphere

TM- 71-1031-3

FILING CASE NO(S)- 105-9

DATE- August 16, 1971

FILING SUBJECT(S)- Planetary Atmospheres
(ASSIGNED BY AUTHOR(S))- Radiative Energy Transfer
Venus Atmosphere

AUTHOR(S)- I. O. Bohachevsky
I. J. Eberstein*

ABSTRACT

In the study of planetary atmospheres two questions are of interest: a) is there global circulation; and if so, b) can it be approximated with a two-dimensional pattern. Developed here is a three-dimensional computer model of an atmosphere heated from one side by the sun that may be allowed to move to account for planetary rotation; it contains two-band absorptivity (visible and infrared) and two effective conductivities (vertical and horizontal) but does not include circulation. Computations carried out for a massive Venus-like atmosphere establish the feasibility of performing three-dimensional calculations of radiative effects. Preliminary observations of the results show that: a) longitudinal and latitudinal pressure variations are substantial; b) pressure and temperature distributions are nonsymmetric with uniform values throughout the dark hemisphere; and c) radiative-conductive relaxation time is comparable to Venusian rotation period. These findings appear to indicate that: a) a realistic treatment of the Venusian atmosphere should contain global circulation; b) because of asymmetry the circulation pattern will not be approximated by a planar two-dimensional model; and c) the analysis should include the effect of planetary rotation. Parametric studies with a one-dimensional version of the program demonstrate the possibility of approximating realistic temperature profiles with a two-band model.

*NRC-NASA Research Associate at Goddard Space Flight Center,
Greenbelt, Maryland.



Bellcomm

955 L'Enfant Plaza North, S.W.
Washington, D. C. 20024

date August 16, 1971
to Distribution
from I. O. Bohachevsky, I. J. Eberstein*
subject Calculation of the Thermodynamic
State of a Three-dimensional Atmosphere
Case 105-9

TM71-1031-3

TECHNICAL MEMORANDUM

I. INTRODUCTION

Previous studies of planetary atmospheres have been concerned, in general, with the determination of vertical profiles of temperature, pressure, or composition at the subsolar point. A flat atmosphere was usually assumed and the effort was directed towards a detailed investigation of the radiative energy transfer between the outer reaches of the atmosphere and the surface. Such studies used elaborate band absorption models and sophisticated scattering theory. General treatment of this subject and references to more special topics may be found, for example, in Refs. 1, 2, and 3.

For some purposes, however, it is desirable to know the complete three-dimensional state of the atmosphere. For example, computation of atmospheric circulation on the global scale requires knowledge of not only vertical but also horizontal temperature distribution. (4,5,6) Also, probes that sent back empirical profiles of the Venusian atmosphere landed on

*NRC-NASA Research Associate at Goddard Space Flight Center,
Greenbelt, Maryland.



the dark side of the planet; to compare with this data, a theory should be capable of predicting vertical distributions of temperature and pressure on the dark side. This can be accomplished by a three-dimensional computation when specification of the surface temperature is inconvenient.

In the present work a method is developed for the treatment of the previously neglected three-dimensional aspect of radiative and conductive-convective heat transfer in a spherically curved atmosphere heated on one side by the sun. A simple two-band absorption model is assumed and different absorption coefficients are used in the visible and infrared portions of the spectrum. The non-isotropic nature of the atmosphere is taken into account by employing different effective eddy conductivity coefficients in the horizontal and vertical directions.

The approach followed is that of numerical time dependent adjustment. In this formulation we begin from an arbitrary temperature distribution and let the computer follow its temporal relaxation to a steady or periodic state. Since three-dimensional time dependent computations are lengthy, our program has also two- and one-dimensional options which should be used when the formulation is such that symmetry properties may be exploited or when the effects of parameter changes on only vertical profiles need be investigated.



The application of the method is illustrated with a computation of three-dimensional temperature distribution in a massive Venus-like atmosphere. The sensitivity of the model to various physical parameters is examined with a sequence of one-dimensional computations. The usefulness and significance of the present computations are indicated by several conclusions inferred from the numerical results.

The memorandum is organized as follows: the "Formulation of the Problem" from which the physical model becomes evident is presented in Sec. II, the "Computational Procedure" is described in Sec. III, and in Sec. IV is presented the list of "Characteristic Parameters" used in the computation together with a brief discussion of each value. Sec. V contains the results together with some preliminary observations and conclusions. In Sec. VI we discuss some possible applications and extensions of the present program.

II. FORMULATION OF THE PROBLEM

In this section we present the mathematical formulation of the problem to be solved. Towards this end we label points in the atmosphere with suitable coordinates as shown in Fig. 1 and develop analytic expressions to describe the physical processes which will occur at each point. From this description will follow the assumptions made to obtain the present simple model.



We consider a planet of surface radius r_s surrounded by a gaseous atmosphere that extends to a maximum radius r_m . A point in the atmosphere is labeled by its: latitude above the equator, ϕ ($0 \leq \phi \leq \frac{1}{2}\pi$), distance from the center of the planet, r ($r_s \leq r \leq r_m$), and longitude, λ . (See Fig. 1.) This convention obtains from a spherical coordinate system modified to conform to the usage of cartographers. The above coordinate system is oriented in such a way that at the time $t = 0$ the sun is located directly above the point $\phi=0, \lambda=0$.

For a rotating planet whose axis is perpendicular to the plane of the orbit, the position of the sun along the equator will subsequently be given by

$$\lambda_s = \omega t ,$$

where ω is the rotation rate and t is time; in order to compute the temperature distribution in this general case all values of λ , $0 \leq \lambda \leq 2\pi$, must be considered. However, in the present memorandum we will treat only the limiting cases of $\omega = 0$ and $\omega = \infty$, i.e., the stationary and infinitely fast rotating planets; they are of interest in themselves and also approximate certain actual conditions. In the non-rotating case no loss of generality results from the restriction of computations to the range $0 \leq \lambda \leq \pi$.



At each point in the atmosphere the rate of change of enthalpy per unit volume ($\rho c_p T$) equals the heat influx to that point, i.e.,

$$\frac{\partial T}{\partial t} = \frac{H}{\rho c_p} = Q \quad (1)$$

where T is the temperature, c_p is the specific heat at constant pressure, ρ is the density, and H is the energy flux.

Eq. (1) may be readily derived from the first Law of Thermodynamics and the assumption that enthalpy changes are independent of pressure, provided that the weight of the atmosphere above any given layer remains very nearly constant; the latter assumption is a widely used standard approximation. It does not mean that the density is constant; ρ will be computed at each time and place from the pertaining values of temperature and pressure.

The rate of temperature equilibration, Q , is composed of three contributions:

$$Q = Q^S + Q^C + Q^Z \quad (2)$$

where the different Q 's represent:



- Q^S - absorption of solar energy
- Q^C - heat addition by a conduction-convection process with an effective conductivity that contains eddy transport
- Q^Z - absorption and re-emission of omnidirectional infrared radiant energy flux.

We now list the explicit expressions for each Q ; these expressions are standard and widely used; therefore we shall indicate their derivations only to bring out the assumptions inherent in each expression.

1. The contribution of the solar flux is:

$$Q^S = \frac{S\alpha}{\rho c_p} e^{-\tau} \quad (3)$$

where:

- a. S is the flux of solar energy at the upper boundary of the atmosphere.
- b. α is the absorptivity assumed equal to $\alpha_{10} \rho$, α_{10} being the absorptivity constant for the visible (more generally, the absorption varies as a power of density but since we are interested primarily in the geometrical effects we take this power to be unity as well as also neglecting the temperature effect),



c. τ is the optical thickness from the point under consideration to the upper boundary of the atmosphere, r_m , measured in the direction of the sun as follows:

$$\tau = \int \alpha dx . \quad (4)$$

2. The contribution of the effective conduction-convection process is:

$$Q^c = \frac{k_r}{\rho c_p} \nabla_r^2 T + \frac{k_h}{\rho c_p} \nabla_h^2 T \quad (5)$$

where:

- a. k_r and k_h are the radial and horizontal effective conductivities
- b. ∇_r^2 and ∇_h^2 are the corresponding components of the Laplacian operator.

The distinction between horizontal and vertical parts of the Laplacian is introduced to account for the different properties of the atmosphere in vertical and horizontal directions.

3. The contribution from the infrared radiant energy flux is:

$$Q^E = \frac{1}{\rho c_p} (A_v - E_v) \quad (6)$$

where A_v is the absorption and E_v emission.



For each frequency ν , A_ν is given by:

$$A_\nu = \alpha \int_0^{2\pi} \int_0^\pi \left[\int_0^x \alpha B e^{-\tau} dx + I_s e^{-\tau s} \right] \sin \psi d\psi d\theta$$

where: $\alpha = \alpha_{30} \rho$ is the absorptivity, α_{30} being the absorption constant for the infrared (see comment about α_{10}),
 B is the Planck's function,
 I_s is the surface energy flux,
 ψ, θ, x are the local spherical coordinates at the given point.

The above expression is rigorously correct for a non-scattering atmosphere and accurately approximates real conditions in many cases (including present) with an appropriate choice of α .

The emission E is given by:

$$E_\nu = \int_0^{2\pi} \int_0^\pi \epsilon B \sin \psi d\psi d\theta$$

where $\epsilon = \epsilon_{30} \rho$ is the emissivity.

As stated in the Introduction, the purpose of the present work is to investigate the three-dimensional geometrical aspect of radiation effects; therefore we will employ the gray gas approximation in the infrared portion of the spectrum. With this approximation:

$$\int_0^\infty B(\nu) d\nu = \frac{\sigma}{\pi} T^4 ,$$



where σ is the Stefan-Boltzman constant and the expressions for absorption and emission become

$$A = \frac{\sigma}{\pi} \alpha \int_0^{2\pi} \int_0^{\pi} \left[\int_0^x \alpha T^4 e^{-\tau} dx + \epsilon_s T_s^4 e^{-\tau_s} \right] \sin\psi d\psi d\theta \quad (7)$$

$$E = \frac{\sigma}{\pi} \epsilon T^4 \quad (8)$$

where the subscript s signifies the surface terms.

To evaluate expressions (3), (5), (7), and (8) that comprise the rate of temperature equilibration it is required to know the thermodynamic equation relating the density, ρ , to the temperature T . Such relation is obtained by introducing a third thermodynamic variable, pressure p . This relation is the ideal gas law

$$p = \frac{R}{M} \rho T \quad (9)$$

where R is the universal gas constant and M is the molecular weight of the gas. Pressure and density are also related by the hydrostatic equation:

$$\frac{\partial p}{\partial r} = -g\rho \quad (10)$$

where g is the gravitational acceleration.

The formulation of the problem described thus far must be complemented with boundary conditions; these are fairly straightforward.



In the case of a non-rotating planet treated in the present work, the atmosphere is symmetric about the equator, $\phi = 0$, and also about the plane passing through the midday and midnight meridians, $\lambda = 0, \lambda = \pi$. This property makes the vanishing of the temperature gradient a suitable boundary condition there.

At the pole, $\phi = \frac{1}{2}\pi$, which is the singular point of the coordinate system, the temperature is set equal to the average value of its horizontal neighbors.

At the upper edge of the atmosphere, $r = r_m$, we prescribe a constant for the ratio $\frac{\partial^2 T}{\partial r^2} / \frac{\partial T}{\partial r}$; the value of this constant is determined from stability and smoothness considerations.

At the lower boundary of the atmosphere which coincides with the surface radius r_s we prescribe the adiabatic condition, i.e., require that the energy flux across the interface between the solid planet and its atmosphere vanishes at each point for all times. Expressed analytically this condition is:

$$-k_s \frac{\partial T}{\partial r} + \sigma \epsilon_s T_s^4 = S e^{-\tau_s} \cos \phi \cos \lambda + \frac{\sigma}{\pi} \int_0^{2\pi} \int_0^{\pi/2} \left[\int_0^x \alpha T^4 e^{-\tau} dx \right] \sin \psi d\psi d\theta. \quad (11)$$

In the above expression $\frac{\partial T}{\partial r}$ is interpreted as $\frac{T_2 - T_1}{2\Delta r}$ where Δr is the radial increment, T_1 is the surface temperature T_s and T_2 is the temperature of the gas adjacent to the surface. With this convention k_s has the same units as k_r and k_h which is useful for comparison purposes.



We wish to point out also that on the part of the surface that is not in the sunlight, $\lambda > \frac{1}{2}\pi$, we set the first term on the right-hand side of Eq. (11) equal to zero.

III. COMPUTATIONAL PROCEDURE

The relaxation of an initial temperature distribution to its equilibrium steady state is governed by Eq. (1). Before presenting the method for numerically following the process described by Eq. (1), however, we must comment about the initial conditions.

The arbitrariness of the initial temperature distribution is limited by the phenomenon known as the "runaway greenhouse effect". It manifests itself through the fact that, for certain combinations of initial conditions and optical properties of the atmosphere, the temperature does not approach a steady state but continually increases beyond all bounds. To guard the lengthy three-dimensional computations against such runaway temperature situations and to make a preliminary comparison of the vertical temperature profile with results of more sophisticated one-dimensional models, it is desirable to verify the choice of initial surface pressure, temperature, lapse rate, and optical characteristics of the atmosphere with a one-dimensional calculation.

The computer program that numerically follows the physical process governed by Eq. (1) is constructed in the following manner. A uniform grid of points separated by distances $\Delta\phi$, Δr , $\Delta\lambda$ is superimposed on the atmosphere. At each point of this grid (ϕ_i, r_j, λ_k) an initial value of the temperature $T_{i,j,k}$ is specified subject to the limitation discussed above. It is



convenient, for example, to prescribe as the initial distribution a constant lapse rate without latitudinal or longitudinal variation.

After the initial temperature field is specified, the boundary conditions are used to extend this field to the set of auxiliary points outside of the boundaries. The temperature array $T_{i,j,k}$ is then advanced one time increment Δt with the finite difference analogue of Eq. (1) which is

$$T^{i,j,k} = T_{i,j,k} + Q_{i,j,k} \Delta t, \quad (12)$$

where the superscripts denote the value at the advanced time. The application of the boundary logic to the advanced array $T^{i,j,k}$ prepares for the next advance. This procedure is repeated until no further change is observed in temperature profiles; clearly this occurs when $Q_{i,j,k} = 0$ at all points.

We now describe the numerical techniques for the evaluation of the different components of $Q_{i,j,k}$.

Prior to the computation of the three parts of Q given by Eq. (2) the pressure $p_{i,j,k}$ corresponding to the current temperature array $T_{i,j,k}$ is computed. The above is accomplished by eliminating the density ρ between Eq. (9) and (10) and integrating Eq. (10) to obtain

$$p_{i,j,k} = p_s \exp \left(-b \int_{r_s}^{r_j} \frac{dr}{T} \right) \quad (13)$$

where p_s is the prescribed surface pressure and $b = \frac{M}{R} g$.



Since the values of $p_{i,j,k}$ vary with altitude by many powers of 10, the integral in expression (13) is evaluated with the Simpson's 1/3 rule for increased accuracy. A comparison of this evaluation with the analytic expression for pressure that can be obtained for a linear temperature distribution reveals that the accuracy is better than 1%.

1. The routine for calculation of solar contribution, Q^S , is constructed as follows. We begin with Eq. (3) in the form

$$Q_{i,j,k}^S = Q_1 e^{-\tau} \quad (3')$$

where the constant $Q_1 = \frac{S_0 \alpha_{10}}{c_p}$. The complication in evaluating (3') is in deciding whether the point (i,j,k) is in the sunlight or shadow and in computing the optical thickness τ .

To determine which points are in the shadow and which in the sunlight we distinguish two regions in the atmosphere:

a. dayside, $0 \leq \lambda_k \leq \frac{1}{2}\pi$ (also $\frac{3}{2}\pi \leq \lambda_k \leq 2\pi$)

b. nightside, $\frac{1}{2}\pi \leq \lambda_k \leq \pi$ (also $\pi \leq \lambda_k \leq \frac{3}{2}\pi$).

All points on the dayside of the planet are in the sunlight; points on the nightside ($\frac{1}{2}\pi \leq \lambda_k \leq \pi$) may be either in the sunlight or in the shadow depending on the value of the product $r_j \sin \phi_i$:

a. when $r_j \sin \phi_i \geq r_s$ the point is in the sunlight



b. when $r_j \sin \phi_i < r_s$ we must, in addition, examine the value of $r_j \cos \phi_i \sin \lambda_k$:

b1. the points with $r_j \cos \phi_i \sin \lambda_k \geq r_s$ are in the sunlight

b2. the points with $r_j (\sin^2 \phi_i + \cos^2 \phi_i \sin^2 \lambda_k)^{\frac{1}{2}} < r_s$ are in the shadow.

For points in the shadow we set $Q^S = 0$; for points in the sunlight we compute τ in the following manner.

At each point (i, j, k) we introduce a local spherical coordinate system (ψ, θ, x) as shown in Fig. 1 in which ψ is measured from the extension of r_j and θ from the azimuthal plane λ_k around r_j . In that coordinate system the direction towards the sun (ψ_s, θ_s) , is:

$$\operatorname{ctg} \theta_s = \operatorname{ctg} \lambda_k \sin \phi_i \tag{14}$$

$$\operatorname{ctg} \psi_s = -\operatorname{ctg} \phi_i \cos \theta_s$$

$$\left. \begin{array}{l} \text{with } 0 \leq \psi_s \leq \frac{1}{2}\pi \\ \pi \leq \theta_s \leq \frac{3}{2}\pi \end{array} \right\} \text{for } 0 \leq \lambda_k \leq \frac{1}{2}\pi$$

$$\left. \begin{array}{l} \text{and } \frac{1}{2}\pi \leq \psi_s \leq \pi \\ \frac{3}{2}\pi \leq \theta_s \leq 2\pi \end{array} \right\} \text{for } \frac{1}{2}\pi \leq \lambda_k \leq \pi$$



With the direction towards the sun determined from (14) the distance along that ray to the edge of the atmosphere, h , is obtained from:

$$h^2 = r_m^2 \cos^2 \phi_m + r_j^2 \cos^2 \phi_i - 2r_m r_j \cos \phi_m \cos \phi_i \cos (\lambda_k - \lambda_m) \quad (15)$$

where

$$\sin \phi_m = \frac{r_j \sin \phi_i}{r_m} \quad 0 \leq \phi_m \leq \frac{1}{2}\pi$$

$$\sin \lambda_m = \frac{r_j \cos \phi_i \sin \lambda_k}{r_m \cos \phi_m} \quad 0 \leq \lambda_m \leq \frac{1}{2}\pi$$

Relations (14) and (15) are obtained from the detailed examination of the geometry involved.

Now, beginning at the point (ϕ_i, r_j, λ_k) we divide the ray (ψ_s, θ_s) into intervals of length Δx and establish the coordinates of the endpoint of each interval from:

$$r^2 = x^2 + 2xr_j \cos \psi_s + r_j^2$$

$$\sin \phi = \frac{r_j}{r} \sin \phi_i + \frac{x}{r} \sin \phi_i \cos \psi_s + \frac{x}{r} \cos \phi_i \sin \psi_s \cos \theta_s \quad (16)$$

$$\lambda = \lambda_k + \lambda_a$$

where $\sin \lambda_a = \frac{x \sin \psi_s \sin \theta_s}{r \cos \phi}$. $-\frac{1}{2}\pi \leq \lambda_a \leq \frac{1}{2}\pi$



At the endpoint of each interval specified by the above coordinates we interpolate among the eight grid points that surround it to determine the pertinent values of temperature $T(x)$ and pressure $p(x)$. With these values and Eq. (9) we can compute the optical thickness from Eq. (4) as follows:

$$\tau = a_1 \sum_{x=0}^{x=h} \alpha_{10} \Delta x \quad (17)$$

where $a_1 = \frac{M}{R} \alpha_{10}$.

With this result Q^S is given directly by (3').

2. The routine to evaluate the effective conductive contribution from Eq. (5) is constructed from the finite difference analogues of the radial and horizontal parts of the Laplacian.

The radial part of the Laplacian in spherical coordinates is given by:

$$\nabla_r^2 T = \frac{\partial^2 T}{\partial r^2} + \frac{2}{r} \frac{\partial T}{\partial r} . \quad (18)$$

The corresponding horizontal part of this operator, however, is singular at the pole $\phi = \frac{1}{2}\pi$. To circumvent any difficulty which this fact may cause during computing, we utilize that property of the Laplacian which states that it is equal to the difference between the average and actual values of the temperature at the point, i.e.,



$$\nabla_h^2 T = \frac{1}{r^2} (T_{av} - T_{i,j,k}) \quad (19)$$

We obtain the average value, T_{av} , from the line integral of T over the surrounding grid points divided by the length of the integration path. In finite difference form it is:

$$T_{av} = \frac{(T_{i-1,j,k} \cos \phi_{i-1} + T_{i+1,j,k} \cos \phi_{i+1}) \Delta \lambda + (T_{i,j,k+1} + T_{i,j,k-1}) \Delta \phi}{(\cos \phi_{i-1} + \cos \phi_{i+1}) \Delta \lambda + 2 \Delta \phi} \quad (20)$$

Substituting (19) and a standard finite difference form of (18) into (5) we obtain:

$$Q_{i,j,k}^c = Q_{2r} \left(\frac{T}{p} \right)_{i,j,k} \left[\frac{T_{i,j+1,k} - 2T_{i,j,k} + T_{i,j-1,k}}{(\Delta r)^2} + \frac{T_{i,j+1,k} - T_{i,j-1,k}}{r_j \Delta r} \right] + Q_{2h} \left(\frac{T}{pr^2} \right)_{i,j,k} (T_{av} - T_{i,j,k}) \quad (21)$$

where:

$$Q_{2r} = \frac{Rk_r}{Mc_p}$$

$$Q_{2h} = \frac{Rk_h}{Mc_p}$$

and T_{av} is given by (20).

3. The routine for the evaluation of the effect contributed by thermal radiation within the atmosphere is based on Eq. (6) in which A and E are given by (7) and (8). For a complete derivation and discussion of these expressions the reader is referred to Refs. 1, 2, or to any standard text on radiative energy transfer.



We will describe presently the process for the computation of absorption A using expression (7). This routine is a generalization of the previously described procedure used to calculate the direct absorption of solar energy. The generalization consists in not restricting the angles ψ and θ (see Fig. 1) to particular values but letting them vary so as to cover the unit sphere: $0 \leq \psi \leq \pi$ and $0 \leq \theta \leq 2\pi$ and computing the emission from all points along each ray (ψ, λ) . For computational purposes ψ and θ assume only a finite set of values ψ_ℓ and θ_n separated by the increments $\Delta\psi$ and $\Delta\theta$.

As a preliminary step to the computation of absorption at the point (i, j, k) we determine the cone generated by rays emanating from that point and tangent to the surface of the planet. It is described by $\psi = \psi_c(r_j)$ with:

$$\cos\psi_c = -\sqrt{1 - \left(\frac{r_s}{r_j}\right)^2} \quad (22)$$

Rays on the outside of this cone, $\psi_\ell < \psi_c$, will not intercept the surface of the planet but will extend to the edge of the atmosphere. Along each such ray (ψ_ℓ, θ_n) we progress with steps Δx whose size depends on the magnitude of changes in the ratio of $\frac{P}{T}$ encountered along the ray. After each step we know the distance along the ray, x , and determine the coordinates (ϕ, r, λ) of the endpoint from Eq. (16) with ψ_s and θ_s replaced



by ψ_ℓ and θ_n , respectively. We interpolate as in the solar routine to determine the values of T and p along the ray; with this information the optical thickness to the point x , $\tau(x)$, is obtained from:

$$\tau = a_3 \int_0^x \frac{p}{T} \Delta x \quad (23)$$

where: $a_3 = \frac{M}{R} \alpha_{30}$.

We continue to increase x until the "edge" of the atmosphere has been reached at $r = r_m$ and then compute

$$A_{\ell,n} = a_3 \int_{\text{all } x} T^3 p e^{-\tau} \Delta x \quad (24)$$

which represents the radiative contribution at the point (i,j,k) from all points along the ray (ψ_ℓ, θ_n) .

The rays inside the cone $\psi = \psi_c$ ($\psi_\ell \geq \psi_c$) terminate at the solid surface of the planet. For these rays it is convenient to compute the total length from:

$$x_s = -r_j \cos \psi_\ell - \sqrt{r_s^2 - r_j^2 \sin^2 \psi_\ell} \quad (25)$$

and to divide this distance into a given number of equal intervals Δx . Then the same procedure as for the previous type of rays, described above, is followed until the summation reaches the solid surface where the surface emission is computed from:



$$A_{se} = T_s^4 \epsilon_s e^{-\tau_s} \quad (26)$$

and added to the expression for $A_{\ell,n}$ given by (24).

The above described calculations are carried out along each ray and the results retained to compute the double sum :

$$A = \sum_{\theta=0}^{2\pi} \sum_{\psi=0}^{\pi} (A_{\ell,n} + A_{se}) \sin\psi_{\ell} \Delta\psi \Delta\theta \quad (27)$$

where the surface emission is added only for $\psi_{\ell} \geq \psi_c$.

The emission at the point (i,j,k) with the grey gas approximation is proportional to

$$E = 4\pi T_{i,j,k}^4 \quad (28)$$

With the values of A and E given by (27) and (28) the radiative contribution composed of absorption and emission at the point (i,j,k) is, from Eq. (6):

$$Q^{\Sigma} = Q_{3A} - Q_{3E} \quad (29)$$

with $Q_{3A} = \frac{\sigma \alpha_{30}}{\pi c_p}$

$$Q_{3E} = \frac{\sigma \epsilon_{30}}{\pi c_p}$$



For radiative equilibrium $\epsilon_{30} = \alpha_{30}$.

The above techniques for the evaluation of derivatives and integrals are employed also to evaluate terms in the boundary condition (11) and to compute the total energy emission from the atmosphere which must balance the energy received from the sun when the steady state is reached.

In the boundary condition (11) the surface temperature T_s is identified with the value of T at the auxiliary points labeled with $j = 1$. It is determined from Eq. (11), which is a quartic, by the Newton-Raphson iteration procedure.

Before closing this section we wish to indicate the modification required to compute solar energy contribution in the case of an infinitely fast rotating planet. In that case it is convenient to imagine that the solar flux is distributed with uniform intensity $\frac{S}{2\pi}$ over a cylinder with a very large radius and the axis parallel to the axis of the planet. At each point in the atmosphere we must sum the solar energy contributions from all directions parallel to the plane of the equator and outside of the cone tangent to the surface of the planet given by Eq. (22). From the geometry of the configuration we derive that each plane parallel to the equator is described by the relation:

$$\cos\theta = - \frac{\cos\psi \sin\phi_i}{\sin\psi \cos\phi_i} \quad (30)$$



Therefore, in the case of an infinitely fast rotating planet, the single ray (ψ_s, θ_s) given by Eq. (14) in the solar routine is replaced with a family of rays such that $0 \leq \psi_s \leq \psi_c$ and corresponding to each ψ_s the θ_s is given by Eq. (30); the total solar energy input at each point is the sum over all above rays.

Of course, in the present case the computations need be performed only for a single meridian plane $\lambda = 0$ and identical distributions assigned for all other values of λ .

IV. CHARACTERISTIC PARAMETERS

In this section we collect for convenience the constants that describe the physical and numerical aspects of our computations.

Numerical examples computed in the present work are intended to approximate conditions in the atmosphere of Venus. Consequently, the relevant values of the physical parameters are taken mainly from Goody and Robinson⁽⁷⁾, NASA SP-8011: "Models of Venus Atmosphere"⁽⁸⁾, and from one-dimensional sensitivity studies described in the next section.

The present section is organized as follows: first are listed the universal physical constants for the sake of completeness, then the parameters that simulate aspects of the Venusian atmosphere, and finally, for convenience, the combinations of the above constants that appear in the program. These listings are followed with the characterization of the mesh used to obtain the results. The c.g.s. system of units is used throughout. The section is concluded with brief comments about values of the physical parameters selected for the present investigation.



A. Universal Physical Constants

- | | |
|--|--|
| 1. Solar constant at .723 AU
Corrected for the Venusian
albedo | $S = .267 \times 10^7 \frac{\text{erg}}{\text{cm}^2 \text{sec}}$ |
| 2. Universal gas constant | $R = .8314 \times 10^8 \frac{\text{erg}}{^\circ\text{K mole}}$ |
| 3. Stefan-Boltzmann constant | $\sigma = .567 \times 10^{-4} \frac{\text{erg}}{\text{cm}^2 \text{ } ^\circ\text{K}^4 \text{sec}}$ |

B. Venusian Characteristics

- | | |
|---|---|
| 4. Surface radius | $r_s = .6050 \times 10^9 \text{ cm}$ |
| 5. Gravitational acceleration | $g = .880 \times 10^3 \frac{\text{cm}}{\text{sec}^2}$ |
| 6. Molecular weight (CO ₂) | $M = .424 \times 10^2 \frac{\text{gm}}{\text{mole}}$ |
| 7. Specific heat at constant
pressure | $c_p = .101 \times 10^8 \frac{\text{erg}}{\text{gm } ^\circ\text{K}}$ |
| 8. Vertical "effective conduc-
tivity" | $k_r = .27 \times 10^{10} \frac{\text{dyne}}{\text{sec } ^\circ\text{K}}$ |
| 9. Horizontal "effective conduc-
tivity" | $k_h = .15 \times 10^{15} \frac{\text{dyne}}{\text{sec } ^\circ\text{K}}$ |
| 10. Absorptivity constant
solar radiation (visible) | $\alpha_{10} = .100 \times 10^{-4} \frac{\text{cm}^2}{\text{gm}}$ |
| thermal radiation (infrared) | $\alpha_{30} = .250 \times 10^{-4} \frac{\text{cm}^2}{\text{gm}}$ |
| 11. Emissivity constant
thermal radiation (infrared) | $\epsilon_{30} = .250 \times 10^{-4} \frac{\text{cm}^2}{\text{gm}}$ |



12. Surface properties

absorptivity in the visible	$\alpha_s = .70$
emissivity in the infrared	$\epsilon_s = .90$
heat conductivity across surface-gas interface	$k_s = .50 \times 10^{14} \frac{\text{dyne}}{\text{sec}^\circ\text{K}}$

13. Surface pressure

$$p_s = .100 \times 10^9 \frac{\text{dyne}}{\text{cm}^2}$$

Above is the complete list of the physical parameters that can be varied at will in the computational program to correspond to the model chosen for investigation. Most of these constants appear in combinations which are computed internally in the program.

The following combinations appear in the computation of:

1. pressure $b = \frac{M}{R}g = .4488 \times 10^{-3}$
2. optical thickness for:
 - a. solar flux $a_1 = \frac{M}{R} a_{10} = .5100 \times 10^{-11}$
 - b. infrared flux $a_3 = \frac{M}{R} a_{30} = .1275 \times 10^{-10}$
3. rate of temperature change due to:
 - a. absorption of solar flux $Q_1 = \frac{S a_{10}}{c_p} = .2643 \times 10^{-5}$
 - b. vertical conductivity $Q_{2r} = \frac{Rk_r}{Mc_p} = .5242 \times 10^8$



- c. horizontal conductivity $Q_{2h} = \frac{Rk_h}{Mc_p} = .2912 \times 10^{14}$
- d. absorption of infrared flux $Q_{3A} = \frac{\sigma_{\alpha} 30}{\pi c_p} = .4467 \times 10^{-16}$
- e. thermal emission $Q_{3E} = \frac{\sigma_{\epsilon} 30}{\pi c_p} = .4467 \times 10^{-16}$

4. energy flux across gas-surface interface

$$F_{2s} = \frac{2S_{\alpha_s}}{k_s} = .7476 \times 10^{-7}$$

$$F_{3s} = \frac{2\sigma}{\pi k_s} = .7219 \times 10^{-18}$$

The mesh used to compute the three-dimensional solution is characterized by the following quantities. The grid extends to $r_m = .620 \times 10^9$ cm (altitude of 150 km) with $\Delta r = .10 \times 10^7$ cm (10 km) for a total of 16 layers. The range of latitudes ϕ , $0 \leq \phi \leq 1/2\pi$, contains also 16 divisions with $\Delta\phi = 6^\circ$, while the longitude λ , $0 \leq \lambda \leq \pi$, is divided by 21 meridians separated by $\Delta\lambda = 9^\circ$. Thus a total of 5376 points is used to describe the state of the atmosphere; to satisfy the boundary conditions additional auxiliary points are employed where needed.

At each meshpoint 40 rays with $\Delta\psi = 30^\circ$ and $\Delta\theta = 45^\circ$ are used to evaluate the contribution of omnidirectional thermal radiation flux. As mentioned previously, the stepsize along these rays, Δx , varies depending on the variation of the integrand:



- c. horizontal conductivity $Q_{2h} = \frac{Rk_h}{Mc_p} = .2912 \times 10^{14}$
- d. absorption of infrared flux $Q_{3A} = \frac{\sigma_{\alpha} 30}{\pi C_p} = .4467 \times 10^{-16}$
- e. thermal emission $Q_{3E} = \frac{\sigma_{\epsilon} 30}{\pi C_p} = .4467 \times 10^{-16}$

4. energy flux across gas-surface interface

$$F_{2s} = \frac{2S_{\alpha} s}{k_s} = .7476 \times 10^{-7}$$

$$F_{3s} = \frac{2\sigma}{\pi k_s} = .7219 \times 10^{-18}$$

The mesh used to compute the three-dimensional solution is characterized by the following quantities. The grid extends to $r_m = .620 \times 10^9$ cm (altitude of 150 km) with $\Delta r = .10 \times 10^7$ cm (10 km) for a total of 16 layers. The range of latitudes ϕ , $0 \leq \phi \leq 1/2\pi$, contains also 16 divisions with $\Delta\phi = 6^\circ$, while the longitude λ , $0 \leq \lambda \leq \pi$, is divided by 21 meridians separated by $\Delta\lambda = 9^\circ$. Thus a total of 5376 points is used to describe the state of the atmosphere; to satisfy the boundary conditions additional auxiliary points are employed where needed.

At each meshpoint 40 rays with $\Delta\psi = 30^\circ$ and $\Delta\theta = 45^\circ$ are used to evaluate the contribution of omnidirectional thermal radiation flux. As mentioned previously, the stepsize along these rays, Δx , varies depending on the variation of the integrand:



the integrand is not allowed to change in one step by more than 50% but must change by at least 15 %. Rays which encounter the solid surface of the planet are divided into an integer number of equal steps in such a way that there are approximately 25 steps in each of them, provided Δx is not outside of the range:

$$\Delta r \leq \Delta x \leq 10 \Delta r.$$

The magnitude of the time increment Δt for a stable computational process cannot be obtained theoretically because of the nonuniform linear spacing between the meshpoints, non-isotropic conductivity, and the presence of nonlinear forcing functions representing the radiation effects. Depending on the values of conductivity, density, and meshpoint separation, the standard stability requirements for the Laplace operator fall anywhere between $\Delta t \leq .55$ sec and $\Delta t \leq .60 \times 10^3$ sec.

In the actual computations we have varied Δt in the range $10 \leq \Delta t \leq 1000$ sec depending on the smoothness of the temperature profiles and the rate at which the dominant term, Q^Z , changed. For purely radiative computations without conductivity effects Δt can be increased by as much as a factor of 100.

Prior to the presentation and discussion of the results we comment about the numerical values of the parameters used in the present investigation.



The values of surface radius, gravitational acceleration, and molecular weight for Venus appear to be generally accepted and require no comments.

The value of specific heat at constant pressure, c_p , is taken from Goody and Robinson (Ref. 7, Table 1) where a representative value of ρc_p is given as $2.7 \times 10^4 \frac{\text{erg}}{\text{°Kcm}^3}$. These authors estimate the vertical and horizontal thermal diffusivities to be 10^4 and $10^{10} \frac{\text{cm}^2}{\text{sec}}$ which, when combined with their value of ρc_p , yield $k_r = .27 \times 10^9$ and $k_h = .27 \times 10^5 \frac{\text{dyne}}{\text{sec}^\circ\text{K}}$. While the absolute magnitudes of these eddy coefficients are difficult to estimate, it appears that their ratio, 10^6 , is unrealistically high; we have reduced it by a factor of nearly 20, resulting in the values listed.

To arrive at a plausible value of the absorptivity constant for solar energy, α_{10} , we utilize the expression for the optical depth of the atmosphere per scale height, $\tau_0 = \alpha_{10} \rho_0 H$, where ρ_0 is the density at the bottom and H is the scale height. Assuming $\tau_0 = .1$ and using the scale height of 15 km in combination with the density $\rho_0 = 1 \times 10^{-1} \frac{\text{gm}}{\text{cm}^3}$ obtained from Ref. 8, p. 12 (high density, minimum solar activity model), we obtain the value listed above.

The value of the absorptivity constant for thermal flux, α_{30} , is set equal to two and one half times the solar energy absorptivity constant to reflect the greater opacity of the Venusian atmosphere to infrared energy flux.



The emissivity constant, ϵ_{30} , is assumed to be equal to the absorptivity constant in accordance with the quasi-equilibrium transport theory ⁽⁹⁾ which we adopt in the present work.

The value of the surface pressure, p_s , for a high density minimum solar activity model of Venusian atmosphere is given in Ref. 8, p. 12 as $.169 \times 10^9 \frac{\text{dyne}}{\text{cm}^2}$. We felt, however, that in view of recent findings ⁽¹⁰⁾ a somewhat lower value of $.100 \times 10^9 \frac{\text{dyne}}{\text{cm}^2}$ (100 atm.) is more realistic. Lower surface pressure is beneficial in another respect which will be discussed presently.

The values of α_{10} and α_{30} appear to be too low for the opacities that are usually associated with the Venusian atmosphere ⁽¹¹⁾. However, one-dimensional computations have shown that with the surface pressure of $.100 \times 10^9 \frac{\text{dyne}}{\text{cm}^2}$, $\alpha_{30} = .25 \times 10^{-4}$ is the highest value which can be used without encountering the previously mentioned runaway greenhouse effect; for lower values of surface pressure a higher value of α_{30} could be used. Apparently the relevant parameter is the optical thickness of a layer of atmosphere having a depth Δr ; this indicates that the effect may be computational.

Another comment about pressure is in order. It may be desirable to integrate the hydrostatic equation from the high altitude edge of the atmosphere down to the surface. This, however, leads to difficulties caused partly by computational reasons. When Eq. (10) is integrated downward, because of the exponential increase of pressure, the absolute pressures at



different points on the surface vary by tens of atmospheres. We believe that such large pressure variations in the longitudinal or latitudinal directions would be incompatible with a realistic atmosphere. Thus, it was assumed that the pressure at the surface was constant and the integration was performed upward.

Values of surface absorptivity and emissivity were chosen to be near unity and to reflect the fact that the surface probably is a more efficient emitter in the infrared frequency range than in the visible. Several neighboring values were also tried without significantly affecting the results.

The use of a single parameter, k_s , to describe heat conductivity across the interface between the atmosphere and the interior of the planet is purely pragmatic. Neither the soil conductivity nor the temperature gradients at both sides of the surface are known. Rather than guess at several unknowns we combine our uncertainty into one effective conductivity parameter k_s . Its value was adjusted during computations in such a way that the surface temperature $T_1 = T_2 + \Delta$, where T_2 is the adjacent gas temperature and Δ is less than 100°K in accord with empirical observations. The required value of k_s turns out to be larger than k_r which is compatible with the fact that the gas temperature gradient used is a mean value over a 10 km slab and therefore lower than the actual value near the surface.



V. PRESENTATION OF RESULTS

We will now present results of a three-dimensional computation and of sensitivity studies with a one-dimensional version of the program. The purpose is to illustrate the type of results obtainable with the computer program described in this memorandum. Some observations and conclusions derived from these results are indicated in the next section.

Before proceeding with the presentation of the three-dimensional temperature and pressure distributions we illustrate the approach to steady state and the resulting vertical temperature profile.

The sequence of curves shown in Fig. 2 represents vertical temperature profiles at the subsolar point ($\phi=0, \lambda=0$) beginning with the initial one (500°K at the surface and 1 deg/km lapse rate) and ending with a distribution that no longer changes as the computations progress. Each profile is labeled with the number of computational cycles performed to reach that state; the same convention will be used also in Figs. 3, 10, and 14. It will be shown later that the temperature inversion near the surface in Fig. 2 is not present for different optical properties of the atmosphere.

The vertical variations of Q^Z and Q^S are shown in Fig. 3. This figure illustrates how the rate of the omnidirectional infrared energy transfer adjusts to become the negative of the solar energy input so that the rate of temperature change vanishes (the effective conductivity contribution is negligible for the conditions of this computation).



The longitudinal variations of temperature at altitudes of 0, 20, and 60 km are presented in Figs. 4 and 5. The temperature decreases monotonically from the subsolar to antisolar meridian and remains essentially constant throughout the dark hemisphere. Thus, the temperature distribution is not symmetric about the terminator.

The longitudinal pressure variations at altitudes of 10, 20, and 110 km are shown in Figs. 6 and 7. Despite the fact that pressure is held constant along the surface of the planet the horizontal pressure gradient on the dayside hemisphere is already significant at the altitude of 10 km and increases monotonically with altitude. The computed pressure gradients are large by meteorological standards; this indicates that in reality there must be a circulation pattern to maintain equilibrium.

Figs. 8 and 9 represent polar cooling and pressure drop, respectively. The thermodynamic state of the atmosphere of a non-rotating planet possesses rotational symmetry about the sun-planet axis and therefore we are in a position to estimate the precision of our computations. The numerical results exhibit the required symmetry (invariance along the terminator) to within 1%.

A comment about the length of computer time required to obtain a three-dimensional solution is in order. One computation of Q^Z 's for all points of the field (over 5000 values) requires approximately 1 hour on the UNIVAC 1108; to perform 100 time advances with varying Q^C and Q^S but constant Q^Z requires approximately 1 hour. In the process of obtaining one solution



we were recomputing Q^z 's every 10 to 100 time steps depending on the rate of change of Q 's and of the solution. Thus a three-dimensional solution required between 100 and 200 hours on the UNIVAC 1108 and a one-dimensional one may be calculated in somewhat less than one hour.

The computing process required over 7200 steps to reach a semblance of the steady state; with the average time step $\Delta t = .3 \times 10^3$ sec this is equivalent to 25 earth days. Such equilibration time is close to the rotation period of Venus (subsolar and antisolar points are interchanged every 60 days) and is indicative of the fact that realistic treatment of the atmosphere should provide for time dependence. The above conclusion has also been reached in Refs. 4 and 5 in connection with a three-dimensional study of the dynamics of Venusian atmosphere.

The physical characteristics of planetary atmospheres are not known with the reliability and accuracy that would render one computation very meaningful. Therefore, parametric studies are needed to assess the sensitivity of the model to various parameters that specify it. In view of the length of time required to complete one solution the sensitivity studies may be most conveniently performed with a one-dimensional version of the program that determines the vertical profile of the atmosphere at the subsolar point. We will now describe results of such investigations. The range of values of different parameters covered in each investigation is indicated on the corresponding figure.



The first computation, shown in Fig. 10, was performed to verify the correctness of the numerical model. From these results we see that in the absence of solar energy flux the temperature distribution becomes constant in space and the atmosphere cools uniformly in time as it should.

The dependence of the temperature profile on the solar constant, S , or, for a given planet, on the atmospheric albedo is shown in Fig. 11. With the diminishing solar constant the curve is not only shifted towards lower temperatures but also exhibits lesser tendency towards temperature inversion near the surface.

The effect of infrared absorptivity, α_{30} , is shown in Fig. 12. This figure also demonstrates the development of the temperature inversion near the surface as the opacity of the medium increases.

The effect of surface pressure, p_s , is shown in Fig. 13. With decreasing pressure both the temperature and the lapse rate decrease.

From results presented in Figs. 11, 12 and 13 we observe that, as mentioned above, the temperature inversion near the surface does not always develop and, as one may expect, it is a combination of the optical thickness and the energy input that produces the runaway greenhouse effect.

The temperature profiles with and without effective conductivity are shown in Fig. 14. We observe that the presence of a conduction mechanism results in warming of the upper layers of the atmosphere.



VI. CONCLUDING REMARKS

The work described in this memorandum: a) has demonstrated the feasibility of performing numerical studies of three-dimensional radiative effects with a two-band absorption model that is capable of approximating realistic vertical temperature profiles and b) has provided some insight into the non-symmetric nature of temperature distribution in a massive Venus-like atmosphere heated from one side by the sun.

Cursory examination of the results obtained with the method formulated here shows that: a) longitudinal and latitudinal pressure variations are substantial; b) pressure and temperature variations are not symmetric about the terminator and have relatively uniform values throughout the dark hemisphere; and c) radiative-conductive relaxation time is comparable to Venusian rotation period. These findings appear to indicate that: a) a realistic treatment of the Venusian atmosphere should contain global circulation; b) because of asymmetry the circulation pattern will not be approximated by a planar two-dimensional model; and c) the analysis should include the effects of planetary rotation.

Preliminary computations with a two-dimensional version of the program have indicated that whenever symmetry properties of the formulation may be utilized (e.g. an infinitely fast rotating planet) the computer time required to obtain a solution decreases by a factor of about 10 to 20.



Parametric studies with a one-dimensional version of the program established the sensitivity of the model to various physical parameters.

Some of the restrictions imposed on the physical model employed in the present investigation may be relaxed with little extra effort. For example, the optical properties of the medium may be programmed as more general functions of density and temperature with hardly any effort at all. Similarly, a more general treatment may be accorded to the equation of state.

The limitation on the resolution of the mesh imposed by the memory capacity of the computing machine may be circumvented by performing computations in layers with the top of one layer serving as the input at the bottom surface of the next layer. We have tried this idea and the preliminary results are promising. An added benefit of such computation is that the optical properties of the medium may be made to depend on the altitude of the layer at no extra cost.

The authors gratefully acknowledge the programming assistance of Mrs. B. J. Brooks; without her dedicated cooperation this work would not have been possible.

I. O. Bohachevsky

I. O. Bohachevsky

I. J. Eberstein

I. J. Eberstein

1031-IOB-lsb
IJE-sje

Attachments
References
Figures 1-14



REFERENCES

1. Goody, R. M., "Atmospheric Radiation, I. Theoretical Basis", Clarendon Press, Oxford, 1964.
2. Elsasser, W. M., "Heat Transfer by Infrared Radiation in the Atmosphere", Harvard Meteorological Studies No. 6, 1946.
3. Pollack, J. B., "Temperature Structure of Nongrey Planetary Atmospheres", *Icarus*, v. 10, pp. 301, (1969).
4. Bohachevsky, I. O., "A Linear Model of Atmospheric Circulation", Bellcomm TM-69-1014-4, January 31, 1969.
5. Bohachevsky, I. O. and Yeh, T. T. J., "General Circulation in the Atmosphere of Venus Driven by Polar and Diurnal Variations of Surface Temperature", Bellcomm TR-69-103-7-2, July 10, 1969.
6. Bohachevsky, I. O., "A Parametric Study of Atmospheric Circulation With a Linear Model", Bellcomm TM-69-1014-6, August 25, 1969.
7. Goody, R. M. and Robinson, A. R., "A Discussion of the Deep Circulation of the Atmosphere of Venus", *Astrophysical Journal*, v. 146, pp. 339-355, (1966).
8. A.S.A. S.P.-8011, "Space Vehicle Design Criteria (Environment) Models of Venus Atmosphere".
9. Lighthill, M. J., "Dynamics of a Dissociating Gas; P.2. Quasi-Equilibrium Theory", *Journ. Fluid Mech.*, v. 8, Part 2, pp. 161-182, (1960).
10. Avduevsky, V. S., Marov, M. Ya., Rozhdestvensky, M. K., Borodin, N. F., Kerzhanovich, V. V., "Soft Landing of Venera 7 on the Venus Surface and Preliminary Results of Investigations of the Venus Atmosphere", *Journ. of Atm. Sciences*, v. 28, No. 2, pp. 263-269, (March 1971).
11. Pollack, J., NASA Ames Res. Ctr. Personal Communication, October, 1970, also Watson, R., Smithsonian Astrophysical Observatory, Cambridge, Mass.

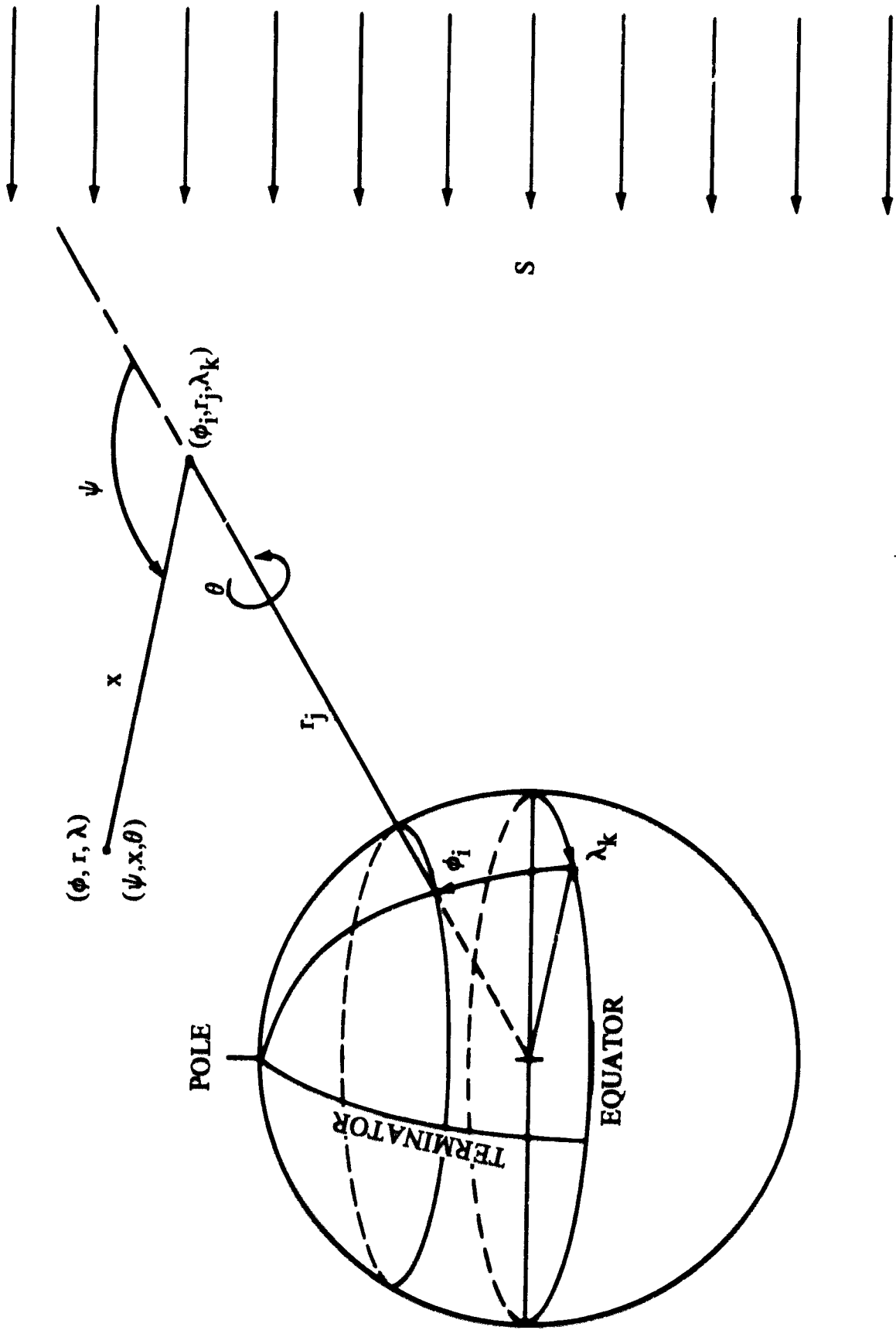


FIGURE 1 - GEOMETRY OF THE PROBLEM AND THE COORDINATE SYSTEM

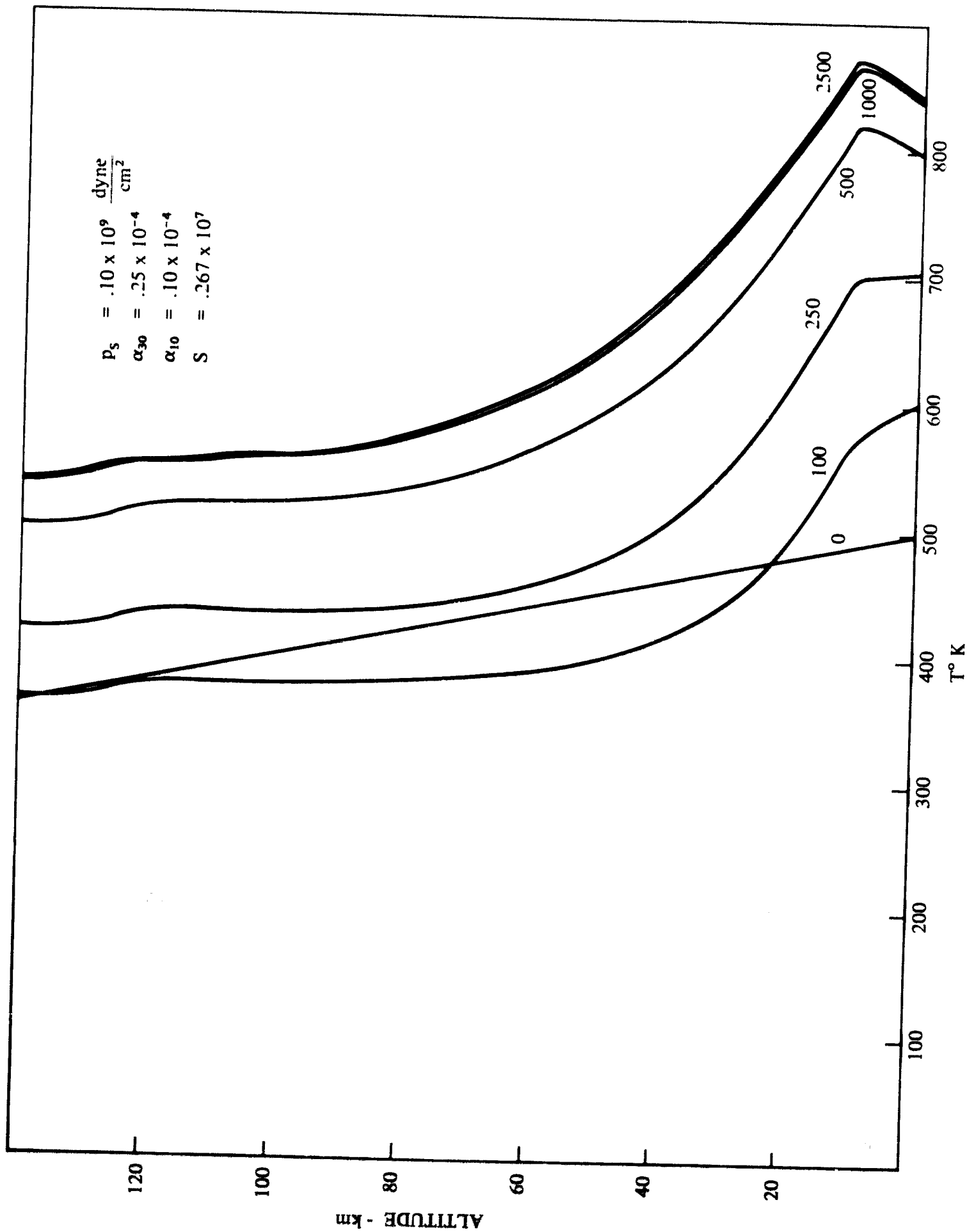


FIGURE 2 - TEMPERATURE APPROACH TO STEADY STATE

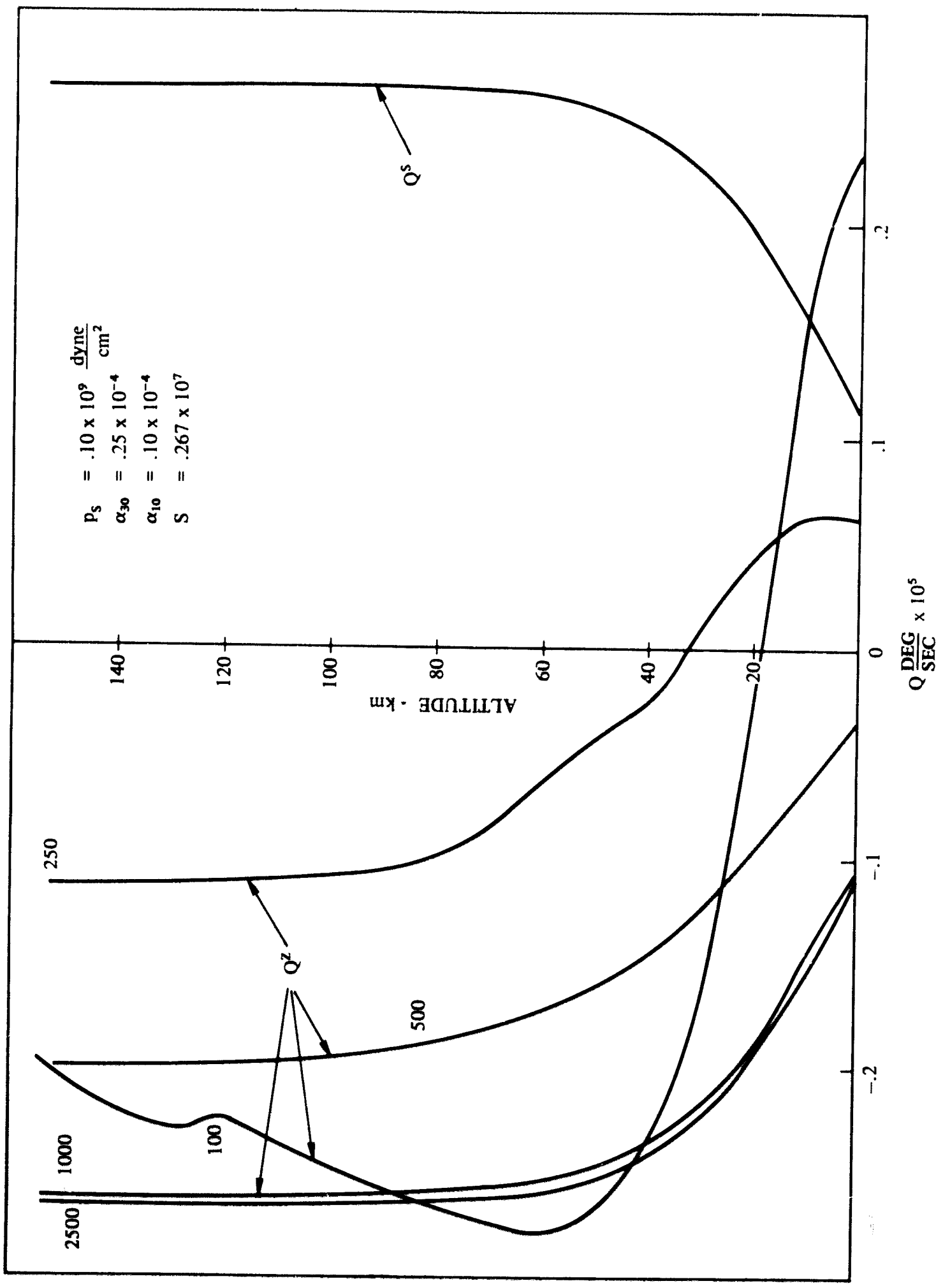


FIGURE 3 - RATE APPROACH TO STEADY STATE

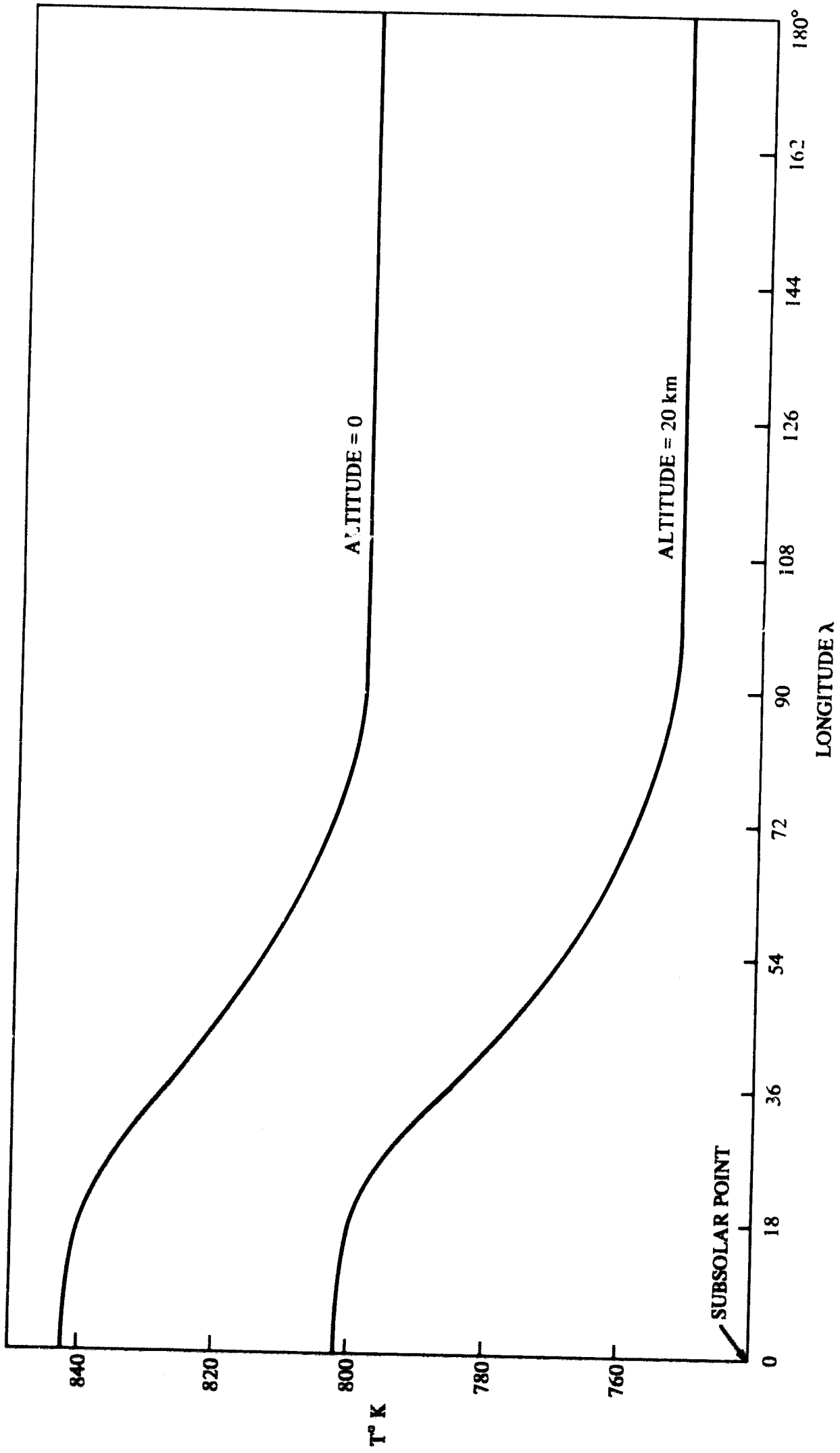


FIGURE 4 - LONGITUDINAL TEMPERATURE DISTRIBUTION (1)

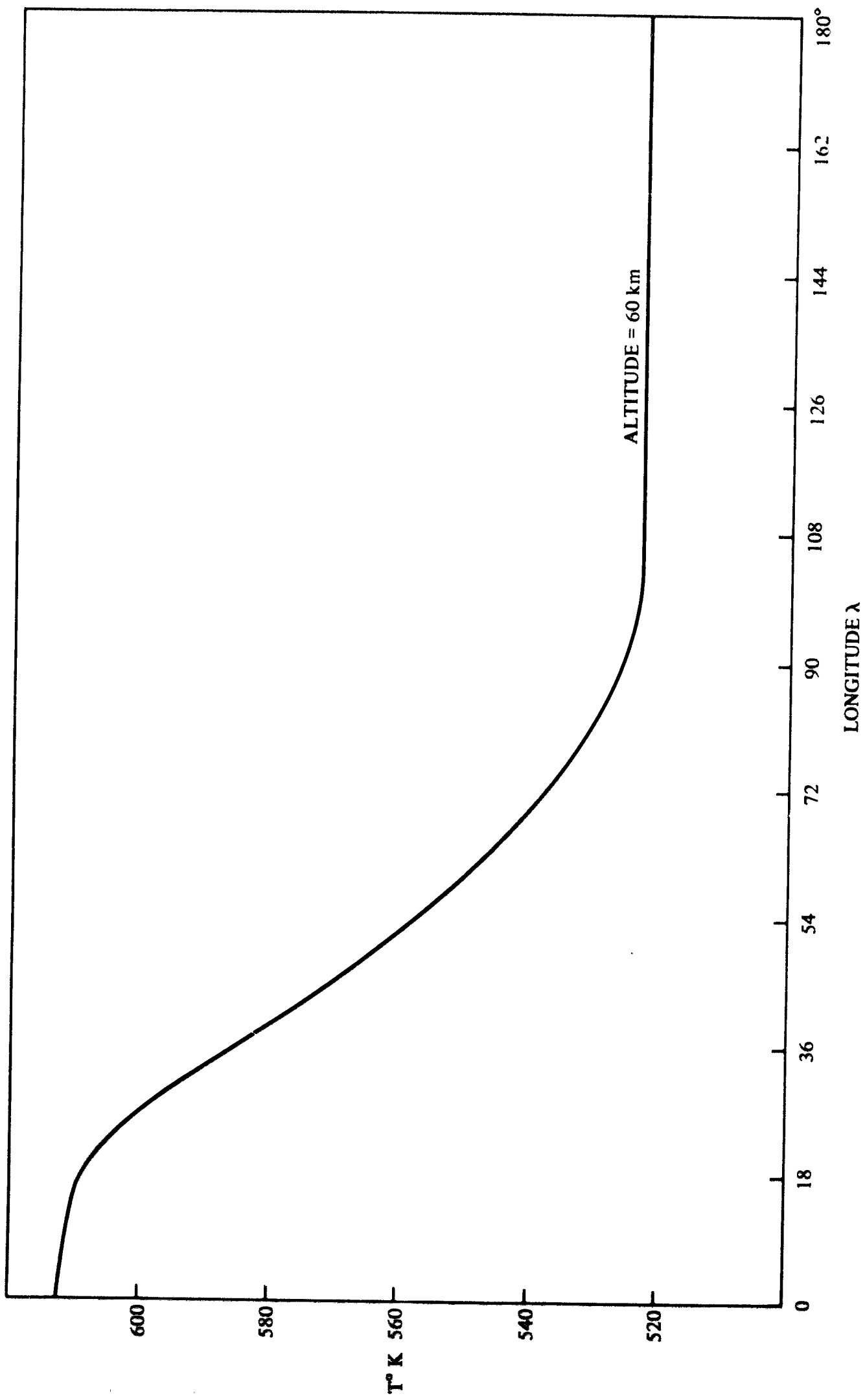


FIGURE 5 - LONGITUDINAL TEMPERATURE DISTRIBUTION (2)

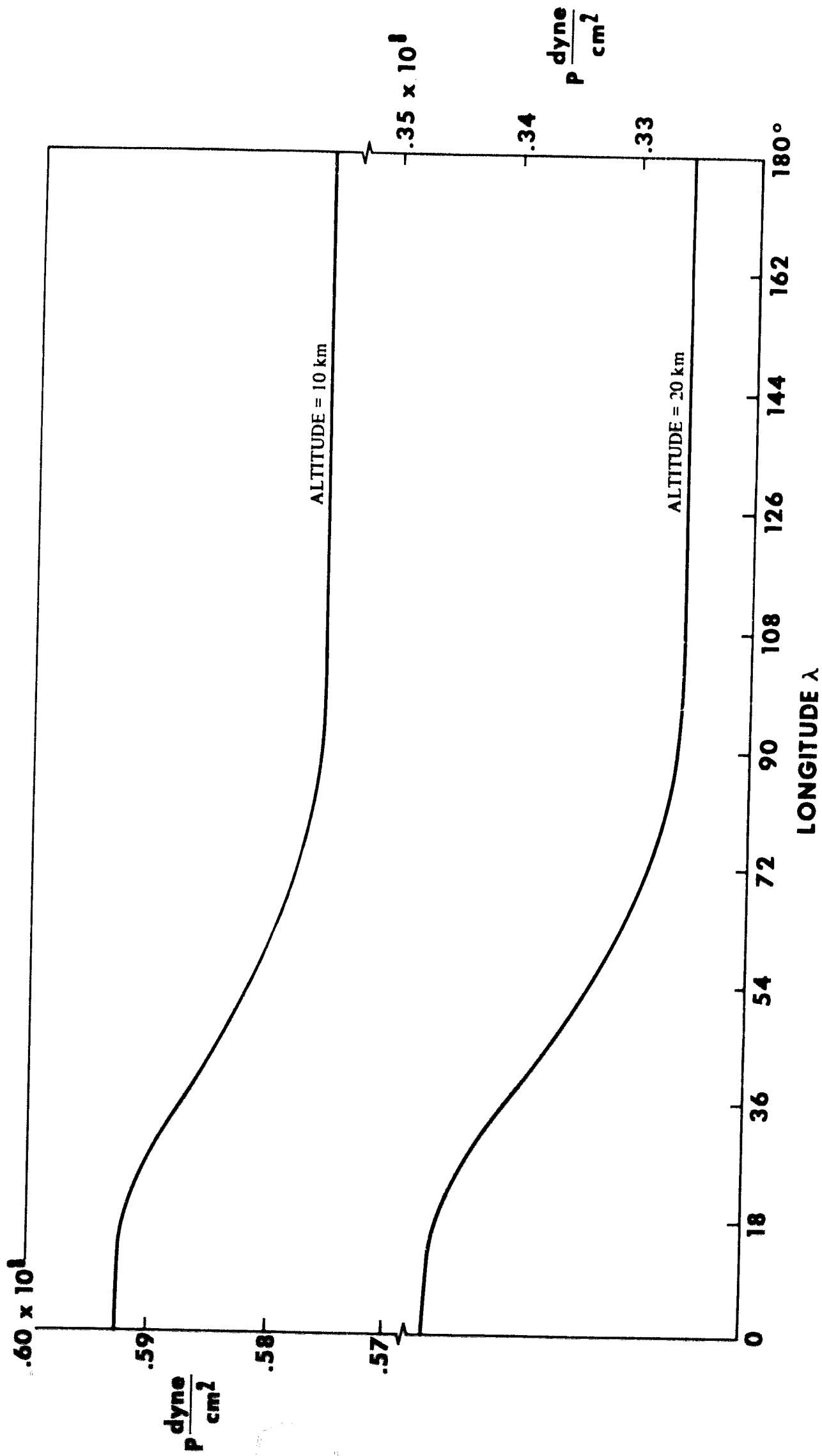


FIGURE 6—LONGITUDINAL PRESSURE DISTRIBUTION (1)

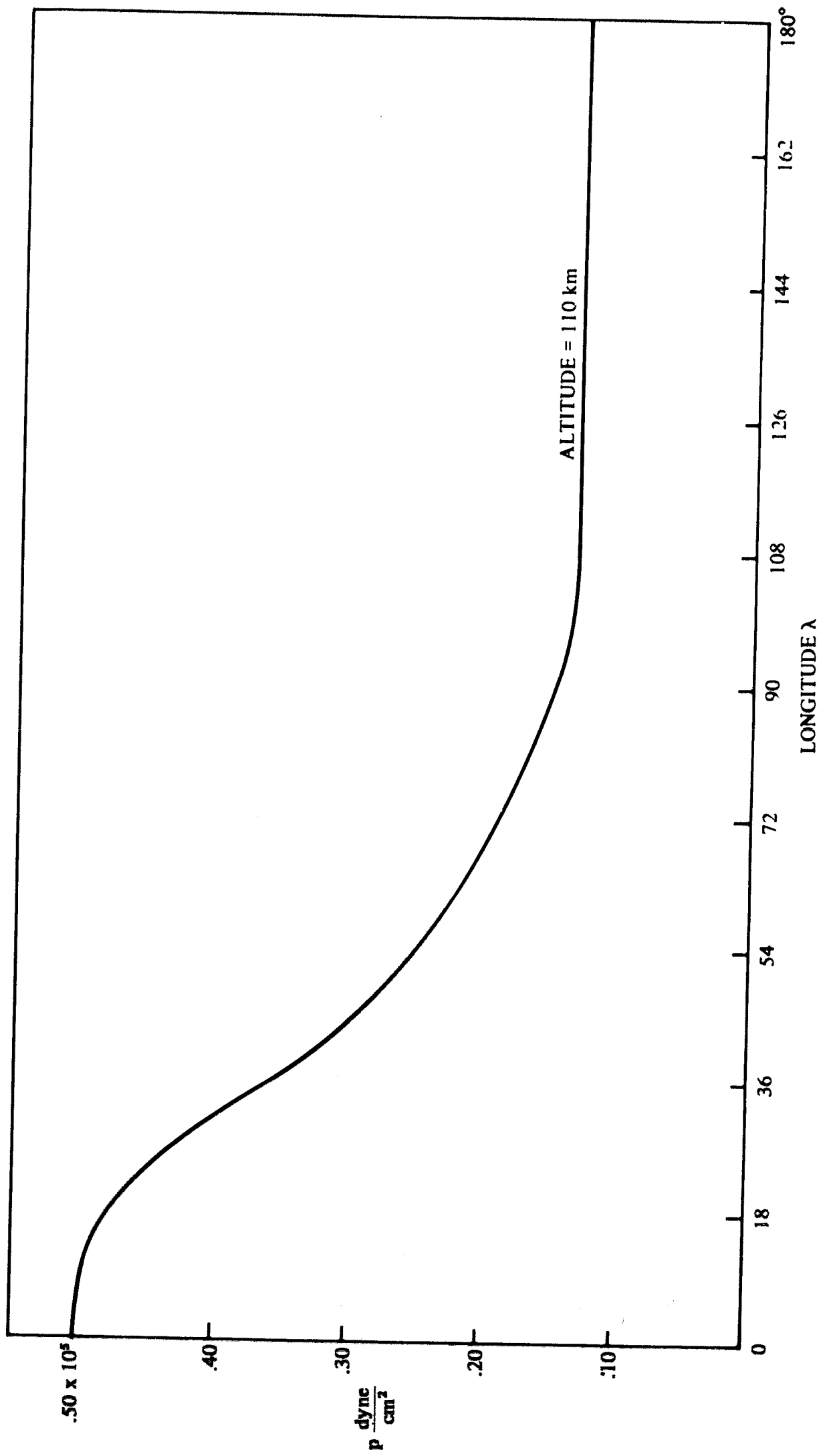


FIGURE 7 - LONGITUDINAL PRESSURE DISTRIBUTION (2)

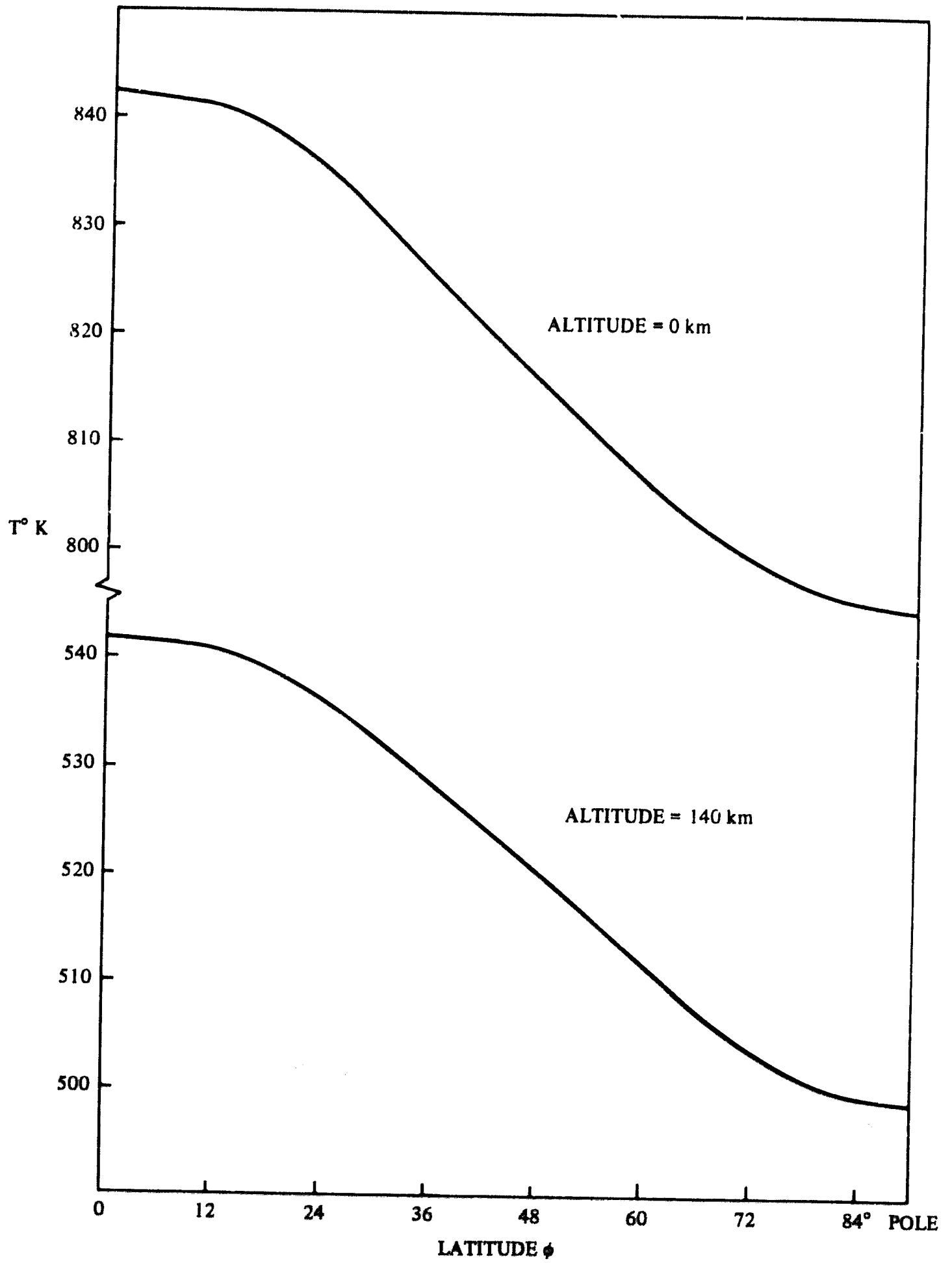


FIGURE 8 - POLAR COOLING

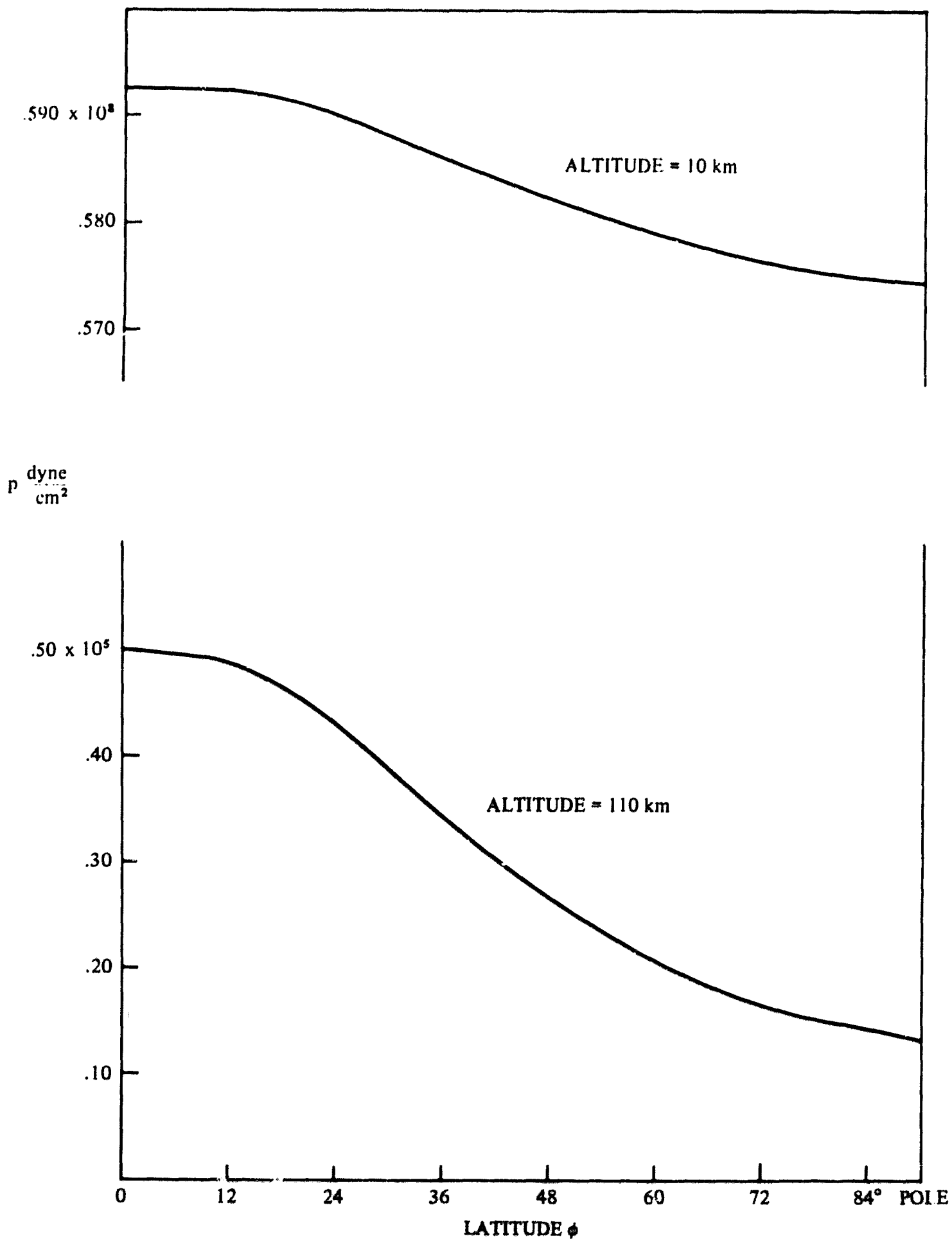


FIGURE 9 - POLAR PRESSURE DROP

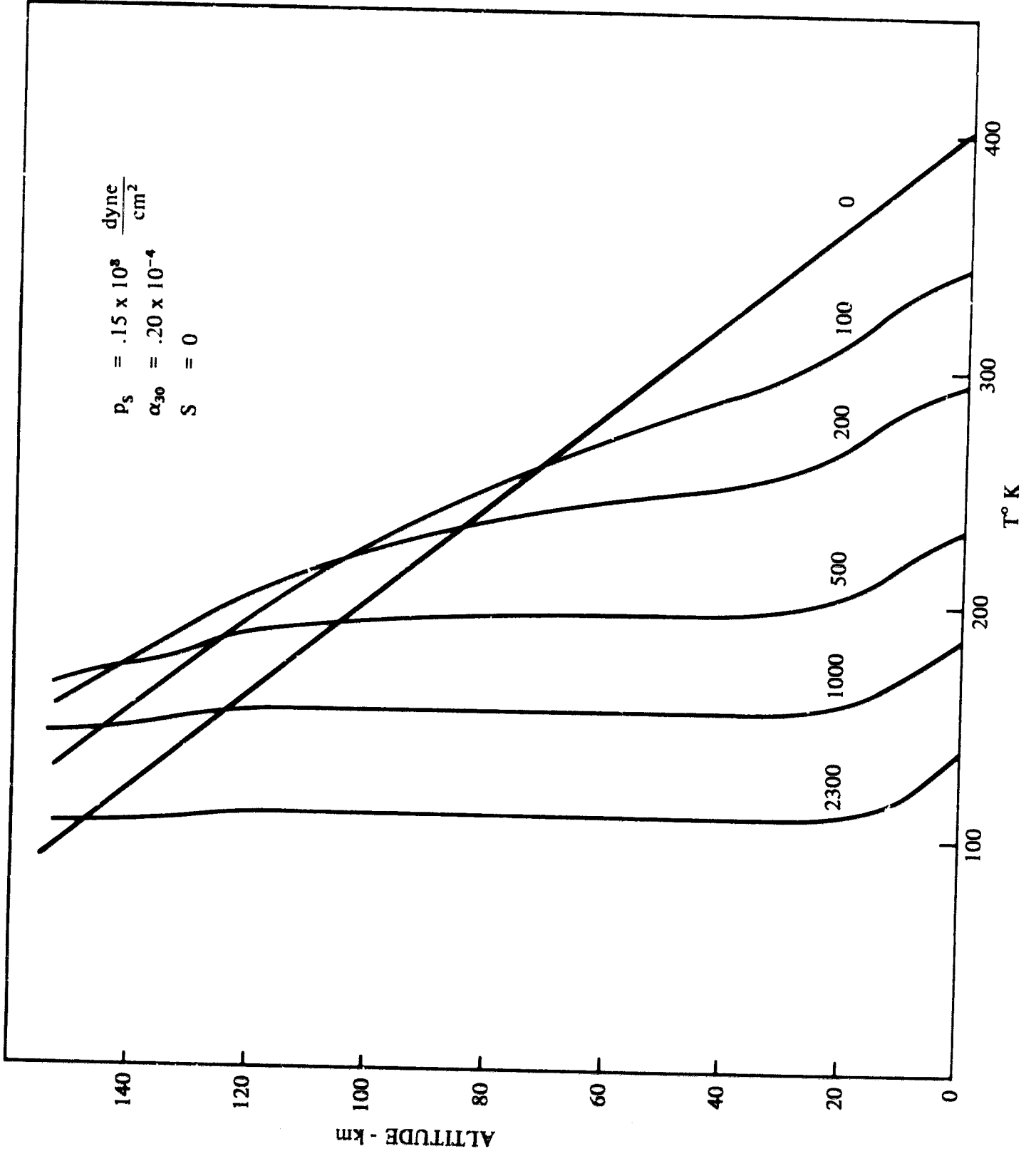


FIGURE 10 - RADIATIVE COOLING OF THE ATMOSPHERE

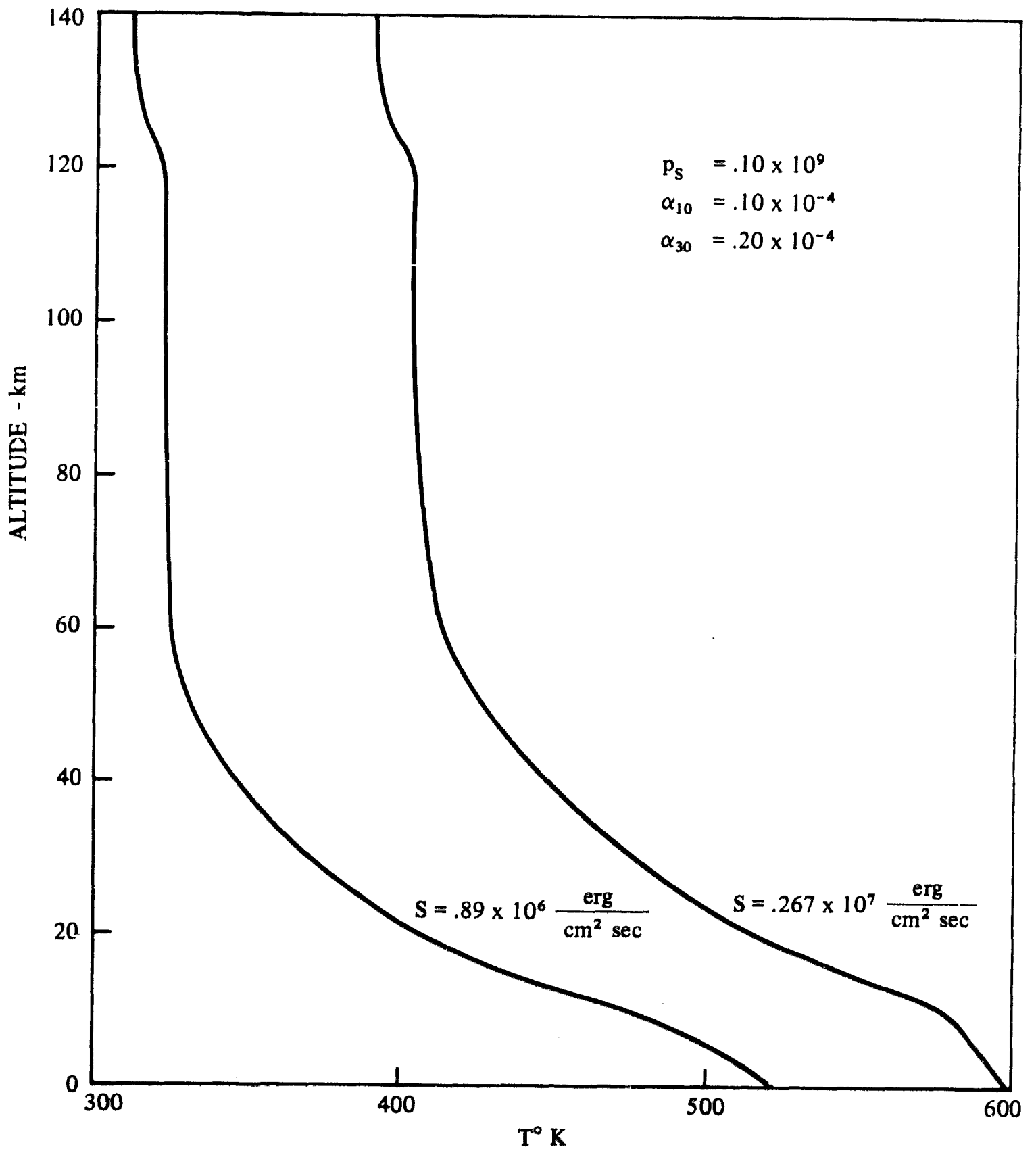


FIGURE 11 - EFFECT OF SOLAR CONSTANT

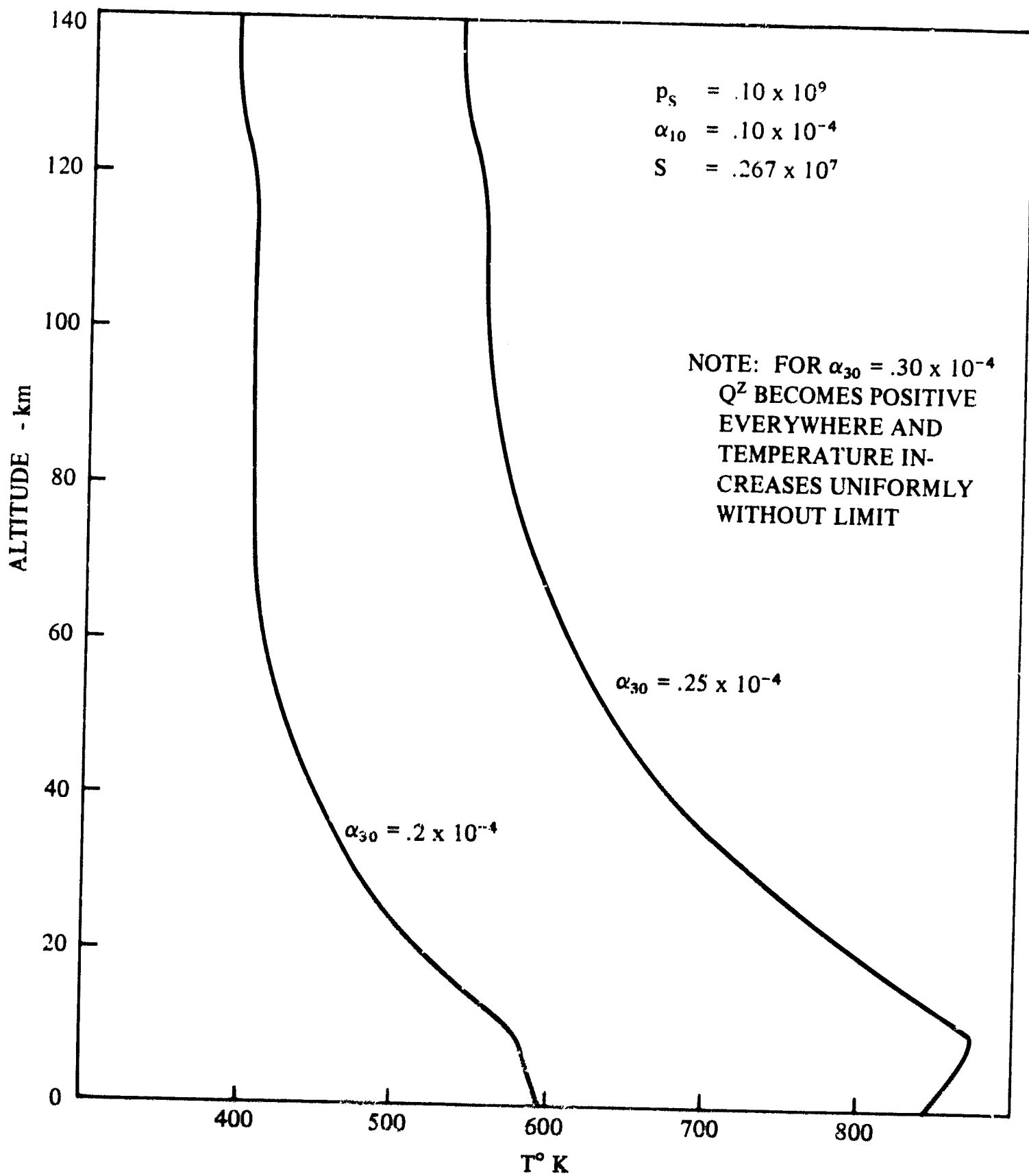


FIGURE 12 - EFFECT OF INFRARED ABSORPTIVITY

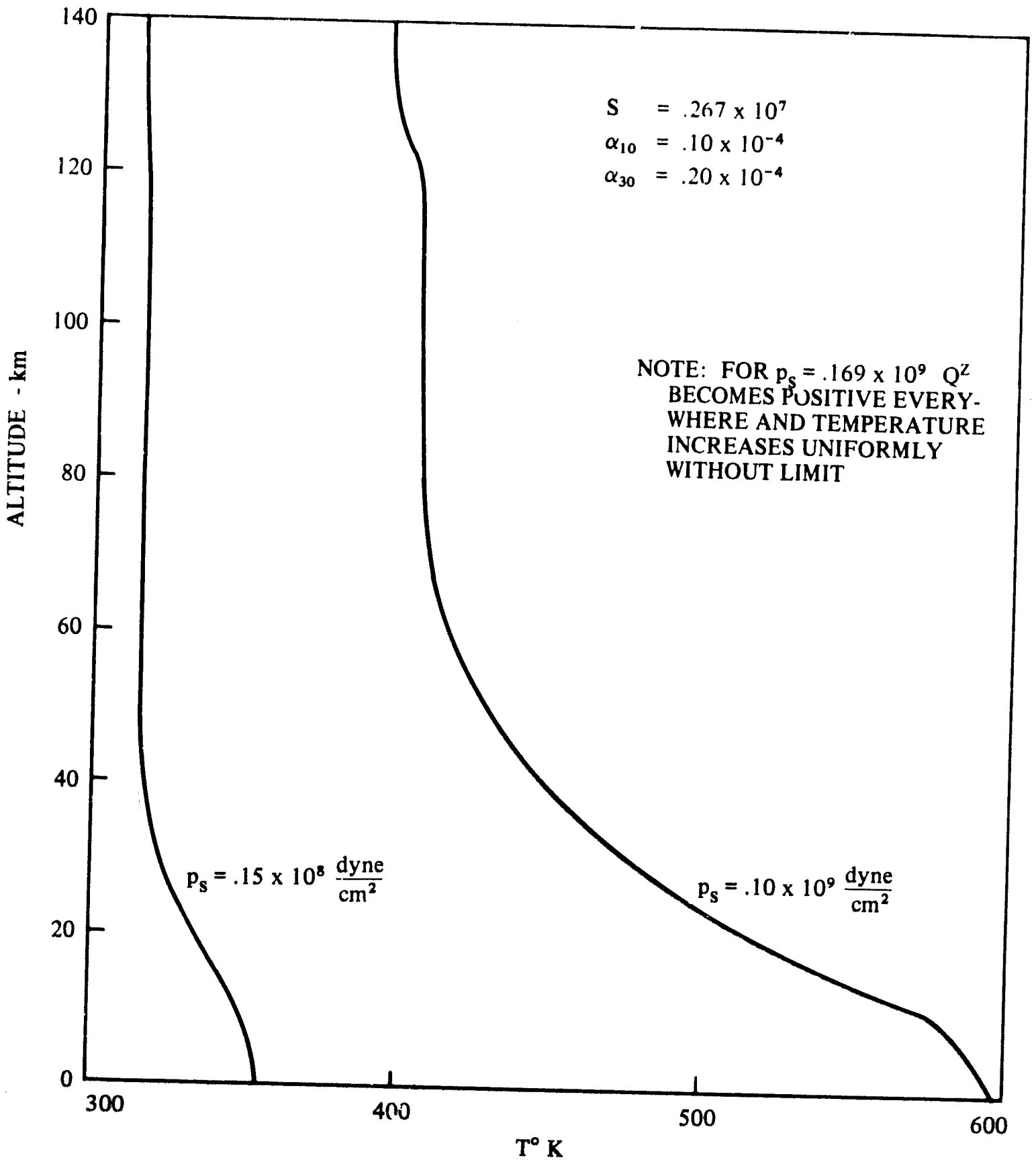


FIGURE 13 - EFFECT OF SURFACE PRESSURE

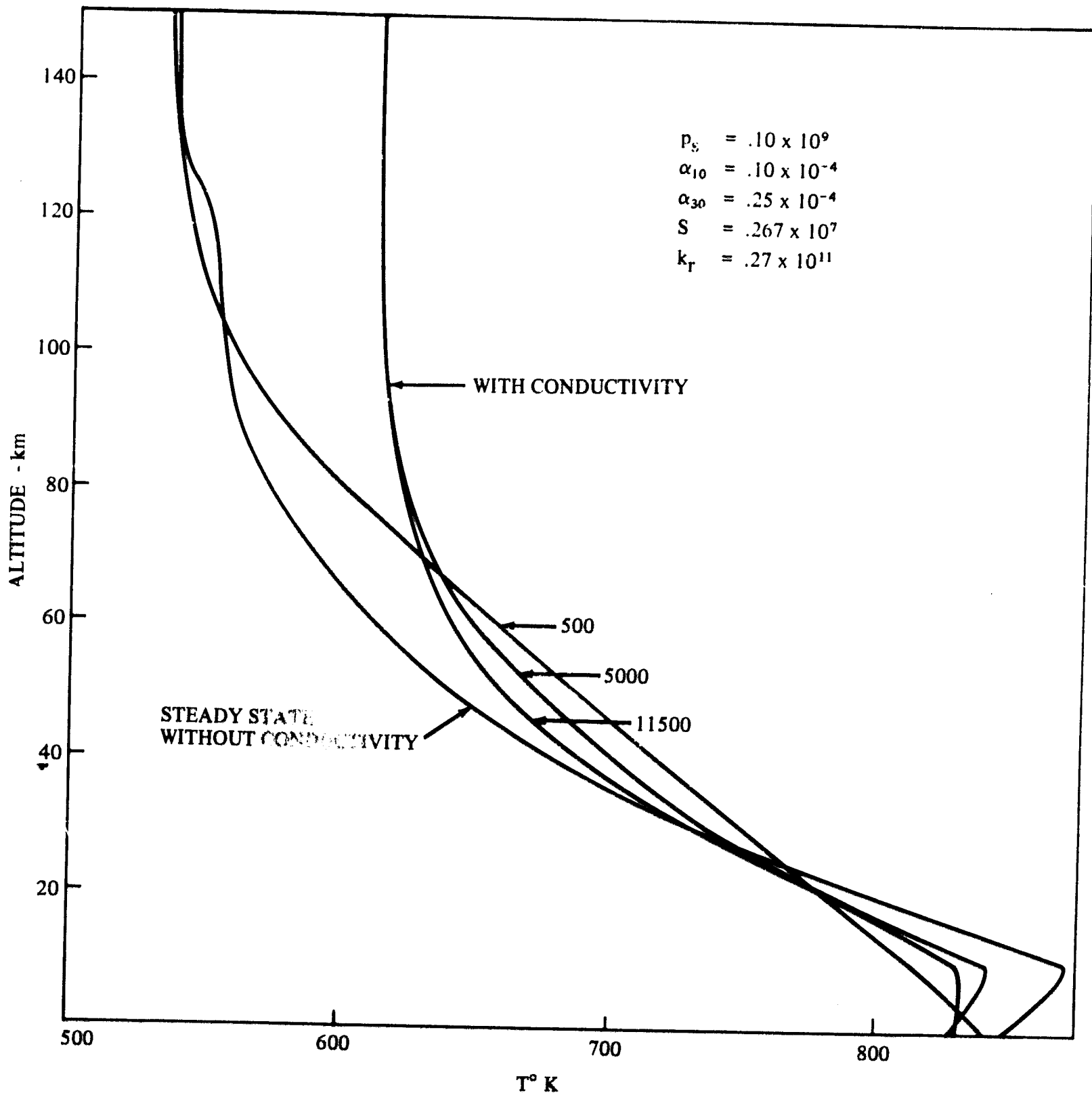


FIGURE 14 - EFFECT OF VERTICAL CONDUCTIVITY